Submitted to Metal Science Journal

UC-25
LBL-8791 c.1
Preprint

INTERDIFFUSION IN TERNARY Co-Cr-Al

G. W. Roper and D. P. Whittle

February 1979

Prepared for the U. S. Department of Energy
under Contract W-7405-ENG-48

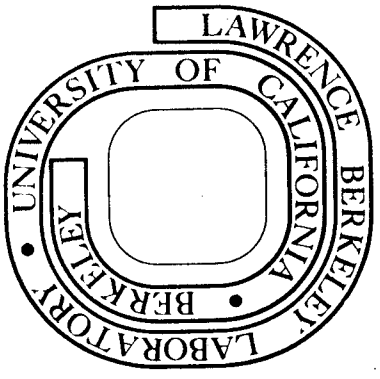

DISCLAIMER

INTERDIFFUSION IN TERNARY Co-Cr-Al ALLOYS

G. W. Roper* and D. P. Whittle**

Department of Metallurgy and Materials Science
University of Liverpool
Liverpool L69 3BX, England

ABSTRACT

The description of interdiffusion in a ternary system requires four composition dependent diffusion coefficients which together form a coefficient matrix. The values of this matrix have been determined for a wide range of compositions in the cobalt solid solution of the Co-Cr-Al system at 1100°C. This was achieved by annealing infinite diffusion couples between appropriate pairs of alloys and then determining the resulting concentration profiles by electron probe X-ray microanalysis.

The figures obtained for the diffusion coefficients were in accordance with expectations based on the results of previous studies of related systems. Furthermore, all four coefficients were found to vary systematically with composition, as illustrated by contour maps. However, this observed variation with composition did not fit theoretical predictions based on the Wagner Dilute Solution Model. Certain anomalous results were explained on the basis of the formation of non-equilibrium vacancy concentrations.

---

* Present address: Shell Research Center, Thornton, Nr. Chester, England.

**Present address: Materials and Molecular Research Division, Lawrence Berkeley Laboratory, University of California, Berkeley, California 94720.

ACKNOWLEDGMENT

This work has been supported by the Science Research Council. G. W. Roper wishes to acknowledge the award of a Science Research Council Research Studentship.

This work is being published with the cooperation of the Division of Materials Sciences, Office of Basic Energy Sciences, U. S. Department of Energy under Contract No. W-7405-Eng-48.

INTRODUCTION

Diffusion in multicomponent systems is fundamentally and significantly different from diffusion in binary alloys. The extra degrees of thermodynamic freedom involved introduces the possibility of interaction between the solute elements, with the result that "uphill diffusion", in which the atoms of a given species diffuse up their own concentration gradient, is possible. This occurs when the gradients of concentration and chemical potential are opposite in sign and it underlines the fact that the driving force for diffusion is activity or chemical potential gradient, rather than concentration gradient. Clearly, under isobaric, isothermal, iso-electric potential conditions, this effect can only be observed in systems of more than two components because in a binary system the chemical potential of each component increases continuously with its concentration making it impossible for chemical potential and concentration gradients to differ in sign.

In practical terms, however, it is still convenient, even in multicomponent systems to formulate diffusion equations in terms of concentration, rather than activity gradients, since this is the experimentally measured parameter, and recent reviews (1,2) of multicomponent diffusion theory summarize the extension of Fick's classical laws of diffusion to multicomponent systems. However, whereas in binary systems only one diffusion coefficient is needed to describe the interdiffusion process, and this is defined in Fick's laws as the ratio between the diffusion flux of one of the two components and its concentration gradient, in a system of n components, $(n-1)^2$ diffusion coefficients are required. These are of two types: direct coefficients which relate the flux of a

component to its own concentration gradient, and indirect or cross coefficients which relate the flux of a component with the concentration gradients of the other components in the system. This clearly makes measurements of diffusion coefficients in even ternary systems somewhat more tedious: at least two separate diffusion experiments are required to obtain the diffusion coefficient data at a single composition point. Nevertheless, in practically important systems, it is desirable that these diffusion measurements are carried out, and the present paper examines diffusional transport in the Co-Cr-Al, a system of considerable practical importance in forming the basis for a number of high temperature superalloys and protective coatings which are now a vital part of gas turbine engine technology.

MEASUREMENT OF DIFFUSION COEFFICIENTS

The usual method of determining diffusion coefficients in a particular system is by analysis of the concentration profiles produced when samples of two alloys of differing compositions are allowed to interdiffuse together at a fixed temperature and for a given time. When the alloy samples are sufficiently thick, general greater than $4\sqrt{Dt}$, where D is the appropriate diffusion coefficient and t the time of the diffusion anneal, the diffusion couple may be regarded as infinitely thick and its end compositions invariant with time. This is the basis of the Boltzmann-Matano method for binary systems (3).

Kirkaldy (4) has shown that the equivalent solution to Fick's diffusion equation for a ternary system is given by:

$$\int_{C_i^-}^{C_i} \frac{x}{V_M}\, dC_i = \frac{-2t}{V_M} \sum_{j=1}^{2} D_{ij} \frac{dCj}{dx} \quad \text{for } i = 1,2 \qquad [1]$$

where C_i is the concentration of component i, C_i^- is the concentration of i at one end of the diffusion couple, x is distance, V_M is molar volume, and the D_{ij}'s are diffusion coefficients in the system in which the third component has been assumed to be dependent. The origin for x, the so-called Matano interface, is defined by writing Equation [1] at $C_i = C_i^+$ (the other end of the diffusion couple) where all the concentration gradients are zero.

$$\int_{C_i^-}^{C_i^+} \frac{x.}{V_M}\, dC_i = 0 \quad \text{for } i = 1,2 \qquad [2]$$

The location of the Matano Interface is a tedious and often inaccurate procedure. Furthermore, if the Molar Volume varies with composition, then the Matano Interfaces defined for each species will not coincide. However, positioning of the Matano Interface can be avoided (5) by a procedure analogous to that used in the analysis of binary diffusion couples (6-8). Introduction of the variable Y_i, such that

$$Y_i = \frac{C_i - C_i^-}{C_i^+ - C_i^-} \qquad [3]$$

allows the integral on the left-hand side of Equation [1] to be replaced by

$$\int_{C_i^-}^{C_i} \frac{x}{V_M} \cdot dC_i - (C_i^+ - C_i^-) \left[(1 - Y_i) \int_{-\infty}^{x} \frac{Y_i}{V_M} \, dx + Y_i \int_{x}^{+\infty} \frac{1 - Y_i}{V_M} \, dx \right] \quad [4]$$

Substitution of Equation [4] into Equation [1] then gives

$$\frac{V_M}{2t} \left(\frac{dx}{dY_i}\right) \left[(1-Y_i) \int_{-\infty}^{x} \frac{Y_i}{V_M} \, dx + Y_i \int_{x}^{+\infty} \frac{1-Y_i}{V_M} \, dx \right] = \sum_{j=1}^{2} D_{ij} \frac{C_i^+ - C_i^-}{C_j^+ - C_j^-} \frac{dY_i}{dY_j} \quad [5]$$

for i = 1,2

Thus, for the ternary Co-Cr-Al, with cobalt as solvent, Equation [5] can be written as

$$\gamma_{Cr} = D_{CrCr} + D_{CrAl} \frac{dC_{Al}}{dC_{Cr}} \quad [6]$$

$$\gamma_{Al} = D_{AlAl} + D_{AlCr} \frac{dC_{Cr}}{dC_{Al}} \quad [7]$$

where

$$\gamma_i = \frac{V_M}{2t} \left(\frac{dx}{dY_i}\right) \left[(1-Y_i) \int_{-\infty}^{x} \frac{Y_i}{V_M} \, dx + Y_i \int_{x}^{+\infty} \frac{1-Y_i}{V_M} \, dx \right] \text{ for } i = Al, Cr \quad [8]$$

Concentration profiles from two different diffusion couples which have a common composition point can then be analyzed, and the set of four equations of the type [6] and [7] solved simultaneously to give the values of the four diffusion coefficients at the common composition point.

EXPERIMENTAL

The starting alloys were prepared by melting together appropriate quantities of cobalt (99.6% wt % pure), chromium (99.5% wt % pure) and aluminum (99.9 wt % pure) in a high frequency vacuum induction furnace. After vacuum casting, the ingots were ground to remove the surface material and then suitably sized blocks, 1 x 1 x 4 cm, were cut from the ingots and each sealed into an evacuated (10^{-2} Torr) quartz tube, together with a piece of tantalum foil to absorb any remaining oxygen at the annealing temperature. The alloy blocks were then homogenized for five days at 1200°C $\pm$ 5°C in a vacuum furnace at a pressure of 10^{-5} Torr.

The compositions of the alloys used were determined by Atomic Absorption Spectroscopy and are listed in Table I. It was necessary to know these as accurately as possible since they were used as standards in the later electron probe x-ray microanalysis.

Samples, 1 x 1 x 0.3 cm, were cut from the homogenized blocks and all six faces ground on SiC papers to remove any surface contamination. One of the 1 x 1 cm faces of each was then polished on diamond impregnated cloth to a finish of 0.25 μm. Diffusion couples were then prepared by binding together two appropriate samples using platinum wire with the two polished faces in contact. This proved to be a more successful

technique than that usually adopted by other workers, namely pressure-welding samples together. The diffusion couples were sealed into evacuated quartz tubes, again with tantalum foil, and annealed in a vacuum furnace at 10^{-5} Torr. The temperature of the diffusion anneal was 1100°C $\pm$ 5°C and the time four days. On removal from the vacuum furnace the quartz tubes were immediately broken open to facilitate rapid cooling of the couples with the object of preserving the high temperature structure of the alloys.

The annealed diffusion couples were sectioned along a plane parallel to the diffusion direction and the sections prepared using standard metallographic techniques. Microscopic examination of the couples indicated that most of the couples were satisfactory: in cases where a clean metallurgical bond had not been formed, a duplicate couple was prepared. There was no evidence of any Kirkendall porosity on any of the couples produced.

Measurement of the concentration profiles across each annealed diffusion couple were carried out using a JEOL JXA 50A electron probe microanalyzer. The diffusion couple was fitted into the microanalyzer using a specially designed jig which ensured that the surface of the couple was flat and that it was correctly aligned with respect to the direction of traverse of the sample under the electron beam. A check on the flatness of the sample was carried out by tuning the spectrometer to the Co. Kα peak with the beam positioned at one end of the diffusion zone and confirming that it remained tuned precisely to the same peak when the sample was moved to the other end of the diffusion zone.

The two spectrometers were then tuned to Cr Kα and Al Kα radiations

respectively and point analysis measurements made at intervals across the diffusion zone with a 20 sec. counting time at each point. Twenty μm intervals were used at the ends of the couple, but these were reduced to 10, 4 and even 2 μm intervals where the x-ray intensity profiles were changing rapidly. Duplicate sets of x-ray measurements were made on every couple analyzed to ensure repeatability.

X-ray intensity data were corrected for background, adsorption, fluorescence and atomic number effects and converted into concentrations using the bulk alloy compositions at the ends of the couple as standards, using a specially designed computer program. The program also calculated and plotted out the diffusion paths.

RESULTS

Table II lists the diffusion couples studied and Figure 1 shows a typical x-ray intensity/distance plot, illustrating the typical amount of scatter in the intensity data. Figure 2 shows the concentration gradients and diffusion path for the same couple (B3). The diffusion path shows the variation of composition across the couple, but generally contains no spatial information. However, this had been remedied in the current presentation by including markers at 20 μm intervals along the diffusion paths. These paths should be time-independent for a given couple, although of course the distance between adjacent markers would depend on annealing time. Essentially, they correspond to increments in the parameter $X\sqrt{t}$ of 3.40×10^{-6} $cm/s^{1/2}$. The spacing of the markers is at its greatest near the central region of the diffusion path and they become increasingly closely spaced as the termini are approached.

The requirement of a mass balance demands that the mean composition of a diffusion couples lies on the straight line between the termini and this demand cannot be satisfied if the diffusion path is wholly to one side of this line. All but two of the couples examined satisfied this requirement, and the exceptions are shown in Figure 3 (couples B6 and B9). The latter does cross the inter-termini line, but there is only a small region of the couple with a composition on the right-hand side.

The only possible explanation for a diffusion path not crossing the inter-termini line is the existence of a non-equilibrium concentration of vacancies within the couple. Generally, in this type of experiment, as indeed in the present work, the potential existence of a vacancy wind (9) is ignored and it is assumed that local sources and sinks are able to maintain the vacancy concentration at its equilibrium value throughout. It must be remembered, however, that the potential for vacancy disequilibrium is particularly serious for the couples B6 and B9 since in each case there is a 20 to 25 wt % step in chromium concentration across the interface counterbalanced by a reverse step of only about 5 wt % in aluminum concentration. Thus, a large flux imbalance is likely with much more material being lost from the chromium-rich side. Under these circumstances, a large excess of vacancies is created on the chromium-rich side and it is not inconceivable that the available vacancy sinks are unable to cope, resulting in a superequilibrium concentration. This would destroy the condition that the diffusion path must cross the inter-termini line.

The problems caused by vacancy disequilibria are likely to be

serious only where large flux imbalances occur. For all the other couples investigated, the diffusion paths display the expected S-shape, and so it may be reasonably assumed that vacancy equilibrium is maintained.

Figure 4 summarizes the diffusion paths for all the couples examined. There are 36 discrete intersections between pairs of diffusion paths and the diffusion coefficient matrix was determined at each using Equations [6] and [7] given earlier. The integrals were determined by a numerical analysis technique using a specially designed computer program: the variation of molar volume with composition was allowed for by assuming Vegard's law. Concentration gradients were also calculated using a numerical analysis technique. Table III presents the calculated values of the diffusion coefficient matrix, together with the pertinent compositions and the pairs of diffusion couples whose diffusion paths provided the relevant intersections.

It must be recognized that some intersection points give more reliable data than others. First, near the termini of couples, the gradients of the diffusion paths ($^{dC}_{Al}/^{dC}_{Cr}$ and its reciprocal) are generally very small and also one or other of the integral terms in both γ_{Cr} and γ_{Al} are small, so that the percentage error in each of these factors is large. Second, where an intersection occurs at a very shallow angle, large errors are introduced into the simultaneous solution of the equations to determine the coefficients, because the difference between the values of the gradients of the two paths ($^{dC}_{Al}/^{dC}_{Cr}$ or $^{dC}_{Cr}/^{dC}_{Al}$) is very small, introducing a large percentage error. Thus, the following values of the diffusion coefficient matrix

are likely to have larger than average percentage errors attached to them:

(i) Intersections 29, 30, 31, 32, 34, and 35 lie within 1 wt % of one of the terminal compositions of one or both of the intersecting diffusion paths.

(ii) Intersections 22, 25, 29, 31, 32, 34, and 35 occur at an acute angle of less than 20°.

DISCUSSION

Confidence in the reliability of the diffusion coefficients in Table III must now be confirmed. Unfortunately, the complex way in which they were determined precludes a quantitative assessment of the confidence limits of each result. Nevertheless, according to Kirkaldy et al (10) the application of thermodynamic and kinetic constraints leads to some restrictions on the allowed values which the diffusion coefficients in a ternary system may take. For the particular system being considered, these may be summarized as:

(a) $D_{CrCr} > 0$ and $D_{AlAl} > 0$

(b) $D_{CrAl} \cdot D_{AlCr} \geqslant 0$

(c) $D_{CrCr} \cdot D_{Alal} - D_{CrAl} \cdot D_{AlCr} \geqslant 0$

Examining Table III indicates that conditions (a) and (c) are always satisfied. However, condition (b) specifies that the product of the cross coefficients must be zero or positive (i.e. both cross coefficients

should have the same sign) and this does not apply to the results at intersections 14, 16, 18, 19, 22, 29, 31 and 34. As indicated earlier, the data from points 22, 29, 31 and 34 may contain large errors since these points are amongst those which lie near the termini of the diffusion paths or have shallow intersections or both. However, there is no obvious source of error in the data from points 14, 16, 18 and 19 and, in fact, there are two features which suggest that the negative cross coefficient product is not an artefact for these four sets of results. First, the compositions of the four points are very similar to one another and second, the negative cross coefficient product is in all cases a result of a negative value of D_{CrAl}.

No definite explanation can be offered for this sytematic non-compliance of these results with condition (b). However, it is interesting to note that the diffusion coefficient matrices at the four intersection points, 14, 16, 18 and 19 (as indeed those of all the intersections except 22 and 34) do meet the conditions imposed on the values of the diffusion coefficients by purely thermodynamic constraints (11) namely,

$$D_{CrCr} + D_{AlAl} > 0 \qquad (d)$$

$$D_{AlAl}D_{CrCr} - D_{CrAl}D_{AlCr} \geq 0 \qquad (e)$$

$$(D_{AlAl} + D_{CrCr})^2 \geq 4(D_{AlAl}D_{CrCr} - D_{AlCr}D_{CrAl}) \qquad (f)$$

Thus, the results obtained at intersections 14, 16, 18 and 19 only fail to meet expectations when kinetic constraints (based on nearest neighbor statistical calculations) are included; that is, conditions (a) to (c) given earlier. Now, the model of diffusion kinetics, on which the

analysis is based, is dependent on the vacancy distribution within the system, the assumption being that an equilibrium concentration of vacancies is preserved at all times. Thus, if a non-equilibrium vacancy concentration arises, the predictions of the kinetic theory, as given by conditions (a) to (c), may be expected to fail. Hence, a possible explanation for the observation of a negative cross coefficient product at certain points in the cobalt solid solution of the Co-Cr-Al system is the establishment of non-equilibrium vacancy concentrations during diffusion anneals, as was discussed earlier in relation to the anomalous diffusion profiles.

Bolze et al (12) have considered the variation of ternary interdiffusion coefficients with composition and, using the Wagner Dilute Solution Model (13), showed that, in dilute solutions, the direct coefficients (D_{CrCr} and D_{AlAl}) are approximately independent of composition, while the cross coefficients are given by

$$\frac{D_{CrAl}}{D_{CrCr}} = \alpha_{CrAl} \cdot C_{Cr} \qquad [9]$$

$$\frac{D_{AlCr}}{D_{AlAl}} = \alpha_{AlCr} \cdot C_{Al} \qquad [10]$$

Figure 5 shows the variation of D_{CrCr} with chromium concentration, excluding the figure determined from intersection 34 which is way out of line with the others, and while there is considerable scatter over approximately half an order of magnitude, an average value of D_{CrCr} has been calculated. This is shown as the horizontal line in Figure 5. A similar procedure for D_{AlAl} is shown in Figure 7 where the scatter is somewhat worse.

Figures 6 and 8 show the variation of D_{CrAl} and D_{AlCr} with chromium and aluminum concentration respectively. In accordance with Equations [9] and [10], these should be linear (assuming that D_{CrCr} and D_{AlAl} remain constant) and the average D_{CrAl}/C_{Cr} and D_{AlCr}/C_{Al} gradients were determined from the values of the gradient defined by each point. The lines of these average gradients are included in Figures 6 and 8.

The average value of the direct coefficients and the average gradients of the cross coefficients are shown in Table IV for reference.

It is apparent from Figures 5 to 8 that the results of the current work do not, in general, fit this simplified theory, and that the scatter about the figures shown in Table IV is substantial. The suggestion that this discrepancy resulted from the quality of the experimental results being poor was dispelled by the discovery that they do in fact vary systematically with composition. To illustrate this, contour maps of each coefficient have been drawn and these are shown in Figures 9 to 12. In all four cases the coefficient values have been shown in units of 10^{-11} cm^2 sec^{-1}.

Thus, all four coefficients are complex functions of both chromium and aluminum concentrations over almost the entire composition range considered. The only exception to this is D_{CrAl} which is approximately independent of aluminum concentration up to about 1.5 wt %. It is apparent then that the Wagner Dilute Solution Model on which the Bolze et al. model is based is not adequate to describe the behavior in this substitutional ternary solution and, until a less restrictive model is available for ternary solid solutions, further analysis of these diffusion coefficient matrices and their variations with composition is

not possible.

It should be pointed out, however, that the Wagner Dilute Solution Model has been more successful in dealing with ternary systems in which one of the solutes is interstitial, including the systems Fe-C-Si (10), Fe-C-Mn (10), Fe-C-Ni (14) and Fe-C-Cr (14). This is to be expected since chemical interactions between the solutes of a dilute ternary system are generally less if one solute is interstitial than if both are substitutional. In particular, the chemical potential of the substitutional solute in a dilute ternary system containing an interstitial solute is very weakly dependent on the concentration of the latter and this is reflected in a very low value of the pertinent cross diffusion coefficient.

In Co-Cr-Al alloys, which are dilute with respect to aluminum, the direct coefficient D_{CrCr} should approximate to the single interdiffusion coefficient of the binary system Co-Cr at the same temperature (and chromium concentration, strictly), while a similar comparison can be made between D_{AlAl} and the single coefficient pertaining to the Co-Al system. Table V compares the measured interdiffusion coefficients in the binary systems, extrapolated to 1100°C, with the two different coefficients of the Co-Cr-Al system. Both D_{CrCr} and D_{AlAl} closely approximate to their respective binary equivalents.

Ternary diffusion coefficients have been measured in the related system Ni-Cr-Al (18) but only at 1150°C. However, by means of the available kinetic data for the binary systems Ni-Cr and Ni-Al these may be extrapolated to 1100°C. Values for a 10 wt % Cr - 2 wt % Al alloy in both systems are compared in Table VI; this composition is approximately

in the center of the single phase α-solid solution for the two systems.

The diffusion behavior of the aluminum in the two systems is very similar since the direct coefficients (D_{AlAl}) are identical while the cross coefficients (D_{AlCr}) are of the same order. In each case D_{AlAl} is an order of magnitude greater than D_{AlCr} and this illustrates that the driving force for diffusion of aluminum in both these systems is completely dominated by the aluminum concentration gradient. The interpretation of this is that the chemical potential of aluminum in these alloys is principally a function of aluminum concentration and virtually independent of chromium concentration. This observation is also consistent with the phase boundary of the primary solid solution running almost parallel to the chromium axis of the phase diagram up to about 30 wt % Cr, which is indicative of a very weak dependence of aluminum potential on chromium concentration (19).

Contrasting with the situation regarding aluminum diffusion, described above, the coefficients relating to the diffusion of chromium (D_{CrCr} and D_{CrAl}) are not the same for the nickel-based system as for the cobalt-based one. In fact, both D_{CrCr} and D_{CrAl} are significantly larger in the former than in the latter. This means that chromium diffuses faster in Ni-Cr-Al alloys than in Co-Cr-Al ones, other things being equal. The binary interdiffusion coefficient in the Ni-Cr system at 1100°C is also markedly greater than that in the Co-Cr system, values being respectively 9.29×10^{-11} and 2.79×10^{-11} cm^2/s.

At the same time it can be seen that D_{CrCr} and D_{CrAl} are approximately equal to each other in each system. Thus, in both cases, the chromium diffusion flux is strongly dependent on both chromium and

aluminum concentration gradients. This may be contrasted with the situation described above concerning the aluminum diffusion flux, which is dominated by the aluminum concentration gradient and is only weakly dependent on the chromium gradient.

Looking at the relative magnitudes of the direct coefficients for the two systems, it is seen that for Co-Cr-Al D_{AlAl} is approximately double D_{CrCr}, while for Ni-Cr-Al the ratio is inverted with D_{AlAl} only about half the value of D_{CrCr}. Of these two results, the former is perhaps to be expected since aluminum has a much lower atomic weight and atomic size than chromium. However, the latter, more surprisingly, result serves to illustrate the fact that these coefficients are not a simple measure of the rate at which atoms jump through the lattice, but include a great deal of information concerning the chemical interactions between all three elements present.

In summary then, it may be stated that the results obtained for the interdiffusion coefficients of the cobalt solid solution of the Co-Cr-Al system are in good agreement with expections, based on the data available for related systems. The direct coefficients D_{CrCr} and D_{AlAl} are similar to the binary interdiffusion coefficients obtained from the systems Co-Cr and Co-Al respectively at the same temperature. Meanwhile, close correlation exists between the coefficients of the Co-Cr-Al system and those pertaining to the related system Ni-Cr-Al, with the exception that D_{CrCr} and D_{CrAl} are both greater in the latter than in the former. This is to be expected, however, from the relative values of the binary interdiffusion coefficients of the Co-Cr and Ni-Cr systems.

REFERENCES

1. J. S. Kirkaldy, Advances in Materials Research, 4 (1970) 55.

2. G. W. Roper and D. P. Whittle, submitted to Int. Met. Rev.

3. L. Boltzmann, Ann. Physik., 53 (1894) 960.

4. J. S. Kirkaldy, Canad. J. Phys. 35 (1957) 435.

5. D. P. Whittle and A. Green, Scripta Met. 8 (1974) 883.

6. F. Sauer and V. Friese, Z. fur Elektrochem. 66 (1962) 353.

7. F. J. A. den Broeder, Scripta Met. 3 (1969) 321.

8. C. Wagner, Acta Met. 17 (1969) 99.

9. J. R. Manning, Met. Trans. 1 (1970) 499.

10. J. S. Kirkaldy and G. R. Purdy, Canad. J. Phys. 40 (1962) 208.

11. J. S. Kirkaldy, D. Weichert and Zia-Ul-Hag, Canad. J. Phys. 41 (1963) 2166.

12. G. Bolze, D. E. Coates and J. S. Kirkaldy, Trans. A.S.M. 62 (1969) 794.

13. C. Wagner, "Thermodynamics of Alloys", Addison-Wesley (1952).

14. L. C. Brown and J. S. Kirkaldy, Trans. A.I.M.E. 230 (1964) 223.

15. J. W. Weeton, Trans. A.S.M. 44 (1952) 436.

16. A. Davin. V. Leroy, D. Coutsouradis and L. Habraken, Cobalt 19 (1963) 51.

17. A. Green, D. P. Whittle, J. Stringer and N. Swindells, Scripta Met. 7 (1973) 1079.

18. A. Green, M. Eng. Thesis, Univ. of Liverpool (1975).

19. G. W. Roper and D. P. Whittle, to be published.

TABLE I

ALLOY COMPOSITIONS

Alloy Number	Nominal Composition wt %	Actual Composition wt %
A1	Co-5Al	Co-5.6Al
A2	Co-5Cr	Co-5.2Cr
A3	Co-5Cr-5Al	Co-3.0Cr-5.3Al
A4	Co-15Cr	Co-11.1Cr
A5	Co-15Cr-5Al	Co-12.3Cr-5.3Al
A6	Co-25Cr	Co-24.4Cr
A7	Co-25Cr-5Al	Co-19.3Cr-4.8Al

TABLE II

SINGLE PHASE DIFFUSION COUPLES

Couple Number	Nominal Composition of Alloys used (wt %) with Alloy Number in Parentheses
B1	Co-5Cr(A2)/Co-5Cr-5Al(A3)
B2	Co-5Cr(A2)/Co-15Cr-5Al(A5)
B3	Co-15Cr(A4)/Co-5Cr-5Al(A3)
B4	Co-15Cr(A4)/Co-15Cr-5Al(A5)
B5	Co-5Cr(A2)/Co-25Cr-5Al(A7)
B6	Co-25Cr(A6)/Co-5Cr-5Al(A3)
B7	Co-5Cr(A2)/Co-5Al(A1)
B8	Co/Co-25Cr-5Al(A7)
B9	Co-25Cr(A6)/Co-5Al(A1)
B10	Co/Co-15Cr-5Al(A5)
B11	Co/Co-5Cr-5Al(A3)

TABLE III

DIFFUSION COEFFICIENT DATA IN Co SOLID SOLUTION OF Co-Cr-Al SYSTEM

No.	Intersecting Diff.	Paths	Composition wt%Al	wt%Cr	D_{AlAl} $cm^2\ sec^{-1}$	D_{AlCr} $cm^2\ sec^{-1}$	D_{CrCr} $cm^2\ sec^{-1}$	D_{CrAl} $cm^2\ sec^{-1}$
1	B4	B5	2.1	11.4	5.4×10^{-11}	1.9×10^{-12}	1.7×10^{-11}	1.9×10^{-11}
2	B4	B6	2.4	11.5	5.6×10^{-11}	7.4×10^{-12}	2.2×10^{-11}	1.2×10^{-11}
3	B4	B8	2.4	11.5	5.6×10^{-11}	6.1×10^{-12}	2.0×10^{-11}	1.3×10^{-11}
4	B4	B9	2.5	11.5	5.7×10^{-11}	6.3×10^{-12}	1.7×10^{-11}	1.4×10^{-11}
5	B5	B6	2.2	12.1	4.9×10^{-11}	5.1×10^{-12}	2.3×10^{-11}	2.4×10^{-11}
6	B5	B9	2.3	12 5	5.2×10^{-11}	5.6×10^{-12}	2.3×10^{-11}	4.1×10^{-11}
7	B5	B8	2.6	13.4	5.5×10^{-11}	1.3×10^{-11}	2.6×10^{-11}	4.7×10^{-11}
8	B6	B8	2.4	11.4	5.2×10^{-11}	6.5×10^{-12}	2.0×10^{-11}	4.5×10^{-12}
9	B8	B9	2.5	11.8	5.9×10^{-11}	6.8×10^{-12}	1.9×10^{-11}	2.7×10^{-11}
10	B3	B8	2.0	7.9	4.3×10^{-11}	5.1×10^{-12}	1.6×10^{-11}	1.4×10^{-11}
11	B3	B10	2.1	7.8	4.2×10^{-11}	4.4×10^{-12}	1.7×10^{-11}	1.8×10^{-11}
12	B2	B3	2.2	7.4	4.6×10^{-11}	5.2×10^{-12}	1.4×10^{-11}	8.8×10^{-12}
13	B2	B8	1.9	6.5	4.4×10^{-11}	4.3×10^{-12}	1.6×10^{-11}	4.3×10^{-13}
14	B2	B10	1.8	6.3	4.6×10^{-11}	2.4×10^{-12}	1.9×10^{-11}	-4.2×10^{-22}
15	B8	B10	1.9	7.1	3.3×10^{-11}	6.1×10^{-12}	1.4×10^{-11}	2.5×10^{-11}
16	B7	B10	1.3	4.1	5.3×10^{-11}	3.3×10^{-14}	1.8×10^{-11}	-3.0×10^{-12}
17	B1	B10	1.5	4.9	4.9×10^{-11}	1.4×10^{-12}	1.9×10^{-11}	9.1×10^{-14}
18	B1	B8	1.7	4.8	5.2×10^{-11}	3.3×10^{-12}	1.7×10^{-11}	-4.5×10^{-13}

TABLE III (contd.)

No.	Intersecting Diff.	Intersecting Paths	Composition wt%Al	Composition wt%Cr	D_{AlAl} $cm^2\ sec^{-1}$	D_{AlCr} $cm^2\ sec^{-1}$	D_{CrCr} $cm^2\ sec^{-1}$	D_{CrAl} $cm^2\ sec^{-1}$
19	B7	B8	1.5	3.8	5.9×10^{-11}	2.6×10^{-12}	1.8×10^{-11}	-1.6×10^{-12}
20	B6	B10	2.8	9.9	5.2×10^{-11}	7.0×10^{-12}	2.4×10^{-11}	1.0×10^{-11}
21	B9	B10	2.8	9.9	5.5×10^{-11}	5.7×10^{-12}	1.8×10^{-11}	2.5×10^{-11}
22	B6	B9	2.8	9.8	3.0×10^{-11}	9.8×10^{-13}	2.7×10^{-11}	-7.6×10^{-11}
23	B2	B9	2.9	9.1	6.1×10^{-11}	6.4×10^{-12}	1.7×10^{-11}	1.7×10^{-11}
24	B2	B6	3.0	9.2	5.8×10^{-11}	8.5×10^{-12}	2.2×10^{-11}	5.0×10^{-12}
25	B1	B11	4.2	2.9	7.5×10^{-11}	-2.1×10^{-11}	1.5×10^{-11}	2.4×10^{-12}
26	B1	B9	4.2	2.9	9.4×10^{-11}	1.4×10^{-11}	2.1×10^{-11}	4.5×10^{-12}
27	B9	B11	4.2	2.9	6.8×10^{-11}	7.3×10^{-12}	2.0×10^{-11}	8.4×10^{-13}
28	B3	B9	4.1	3.3	1.0×10^{-10}	1.7×10^{-11}	2.1×10^{-11}	6.2×10^{-12}
29	B3	B11	4.5	3.0	7.2×10^{-11}	-8.0×10^{-11}	9.9×10^{-12}	8.8×10^{-13}
30	B2	B7	0.3	5.1	4.0×10^{-11}	-1.5×10^{-11}	2.4×10^{-11}	-2.0×10^{-12}
31	B1	B2	0.4	5.2	4.4×10^{-11}	-1.6×10^{-11}	1.9×10^{-11}	2.3×10^{-12}
32	B3	B4	0.3	11.1	2.4×10^{-11}	8.7×10^{-12}	2.6×10^{-11}	1.0×10^{-11}
33	B7	B11	2.6	2.2	7.1×10^{-11}	9.0×10^{-13}	3.0×10^{-11}	4.0×10^{-13}
34	B4	B10	4.3	12.0	7.7×10^{-11}	-1.7×10^{-11}	9.7×10^{-11}	1.9×10^{-11}
35	B2	B4	4.6	12.1	2.7×10^{-11}	1.3×10^{-10}	3.7×10^{-11}	1.1×10^{-12}
36	B3	B5	1.7	8.7	3.3×10^{-11}	3.0×10^{-12}	1.1×10^{-11}	4.7×10^{-12}

TABLE IV

AVERAGE VALUES OF DIFFUSION COEFFICIENT DATA FOR THE Co-Cr-Al SYSTEM AT 1100°C

D_{CrCr}, cm^2/s	D_{CrAl}/C_{Cr} $cm^2/s/wt\ \%$	D_{AlAl}, cm^2/s	D_{AlCr}/C_{Cr} $cm^2/s/wt\ \%$
2.0×10^{-11}	1.2×10^{-12}	5.4×10^{-11}	3.2×10^{-12}

TABLE V

COMPARISON OF INTERDIFFUSION COEFFICIENTS AT 11°C (cm^2/s)

		Reference
D in Co-Cr	3.3×10^{-11}	(15)
	1.9×10^{-11}	(16)
	3.2×10^{-11}	(17)
D_{CrCr}	2.0×10^{-11}	present work
D in Co-Al	5.3×10^{-11}	(18)
D_{AlAl}	5.4×10^{-11}	present work

TABLE VI

COMPARISON OF THE DIFFUSION COEFFICIENT MATRICES OF Ni 10 WT % Cr 2 WT % Al AND Co 10 WT % Cr 2 WT % Al AT 1100°C

	D_{CrCr} $cm^2\ sec^{-1}$	D_{CrAl} $cm^2\ sec^{-1}$	D_{AlAl} $cm^2\ sec^{-1}$	D_{AlCr} $cm^2\ sec^{-1}$
Ni 10 wt % Cr 2 wt % Al	9×10^{-11}	1×10^{-10}	5×10^{-11}	2×10^{-12}
Co 10 wt % Cr 2 wt % Al	2×10^{-11}	1×10^{-11}	5×10^{-11}	6×10^{-12}

Figure 1 :- Al Kα and Cr Kα X-ray Intensity Profiles across Diffusion Couple B3

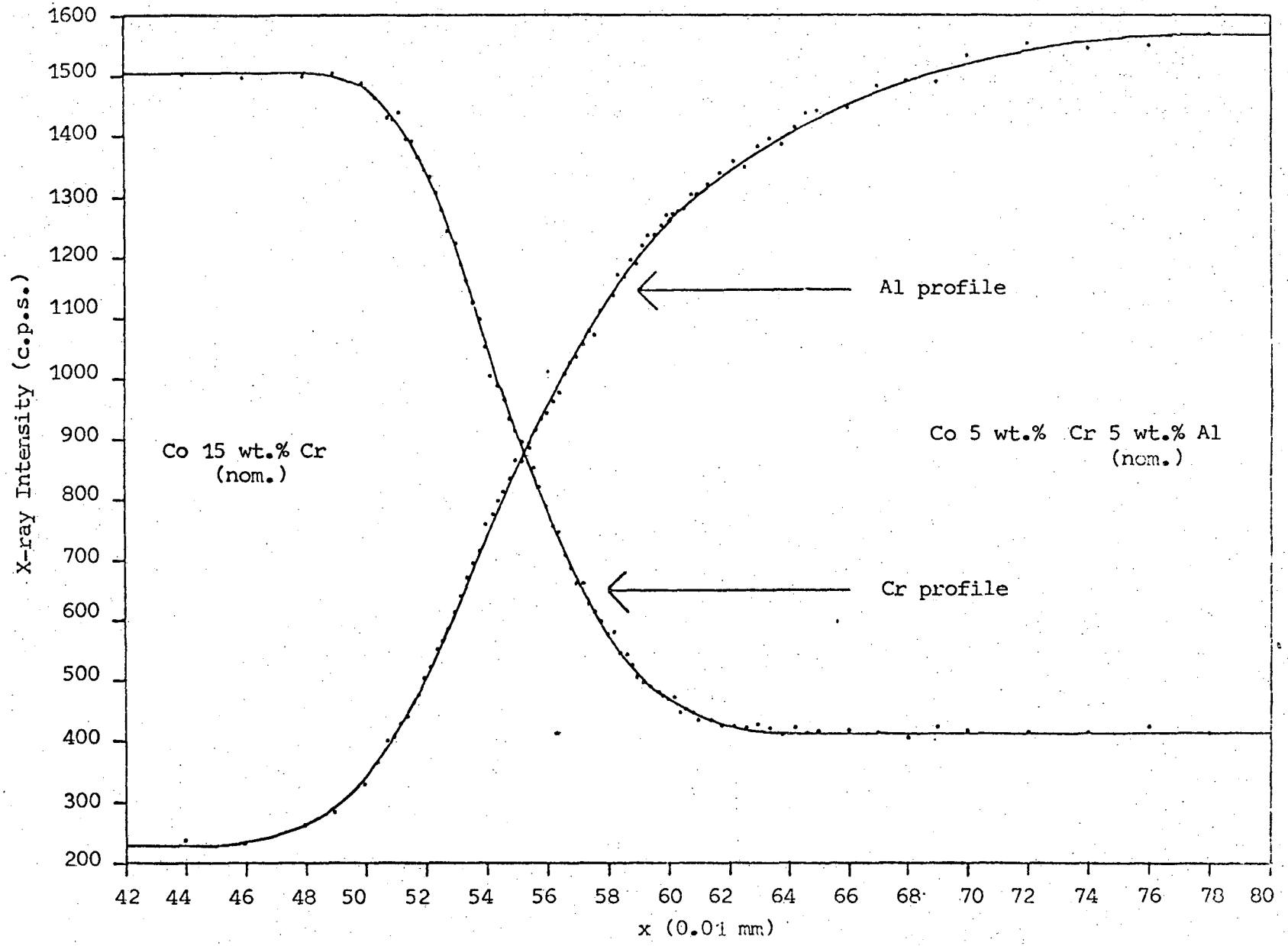

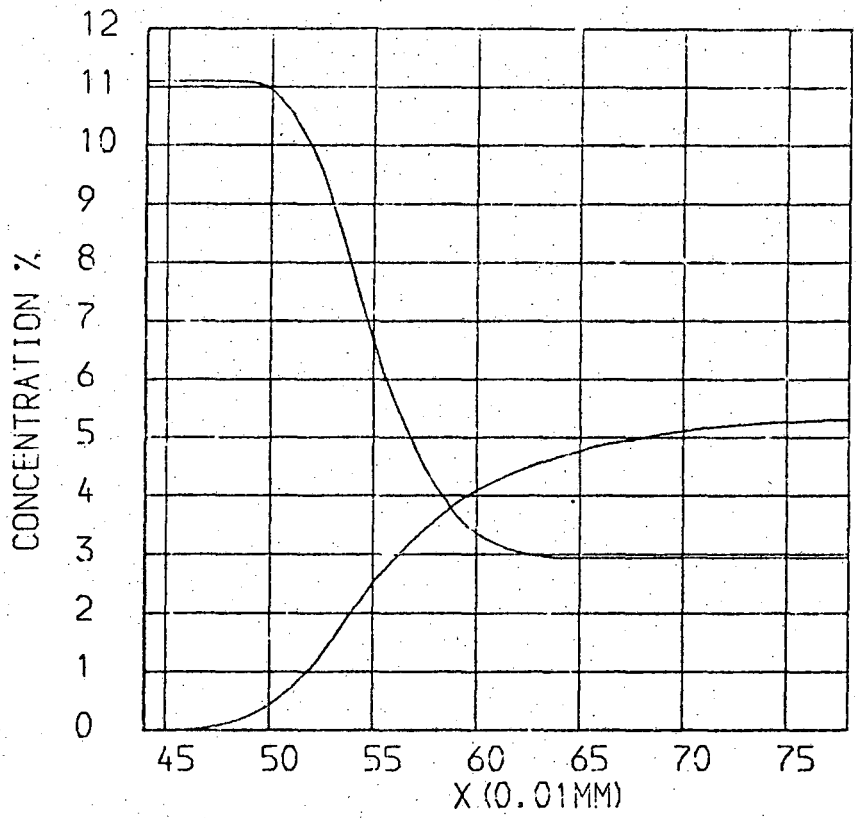

FIG. 2(a) : Aluminium and Chromium Concentration Profiles across Couple B3 (Co 11.1wt.%Cr - Co 3.0wt.%Cr 5.3wt.%Al)

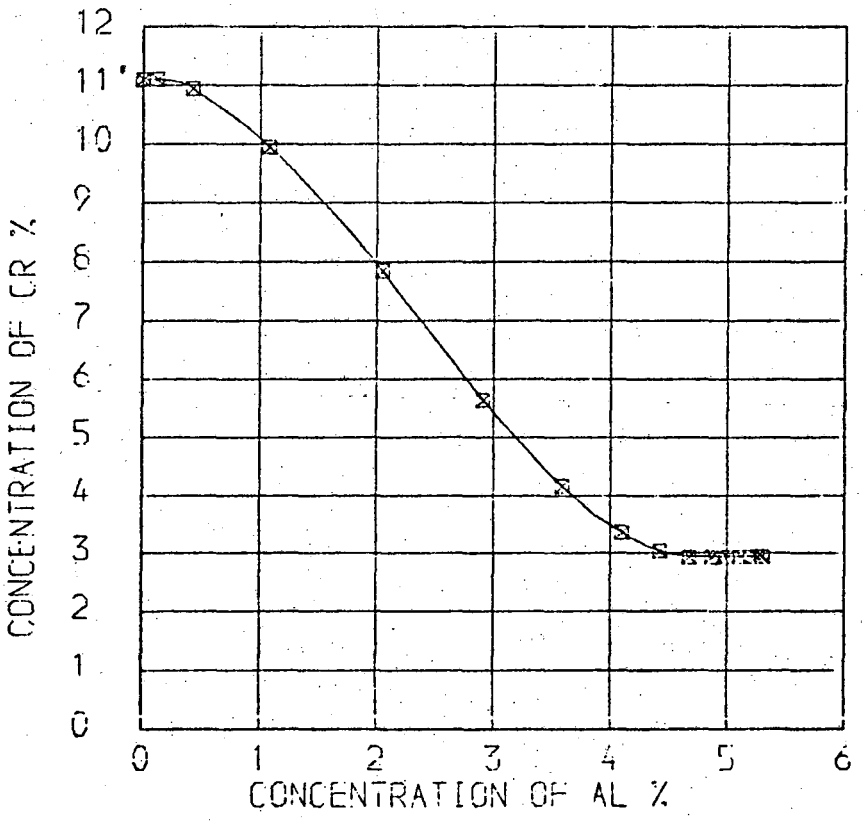

FIG. 2(b) : Diffusion Path of Couple B3.

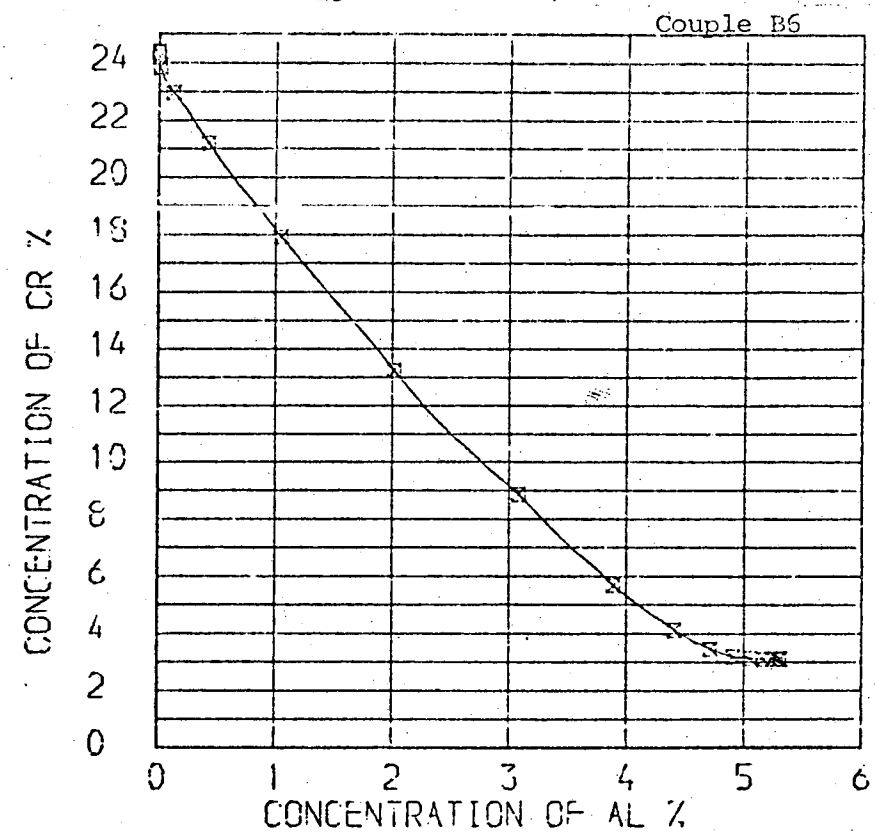

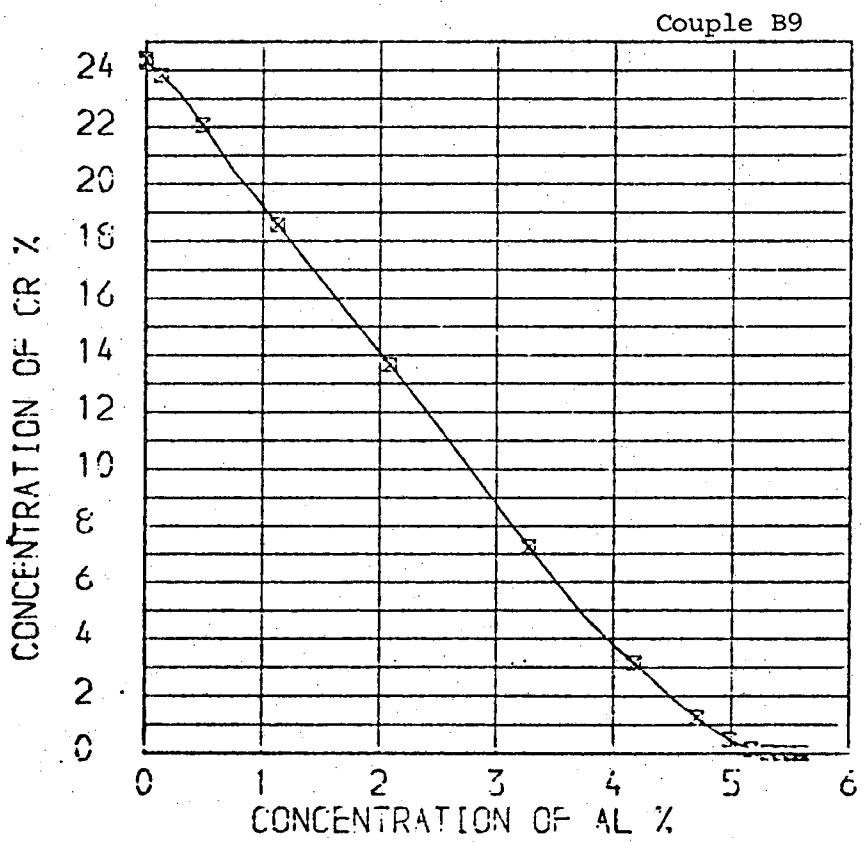

FIG. 3 : Diffusion Paths of Couples B6 and B9.

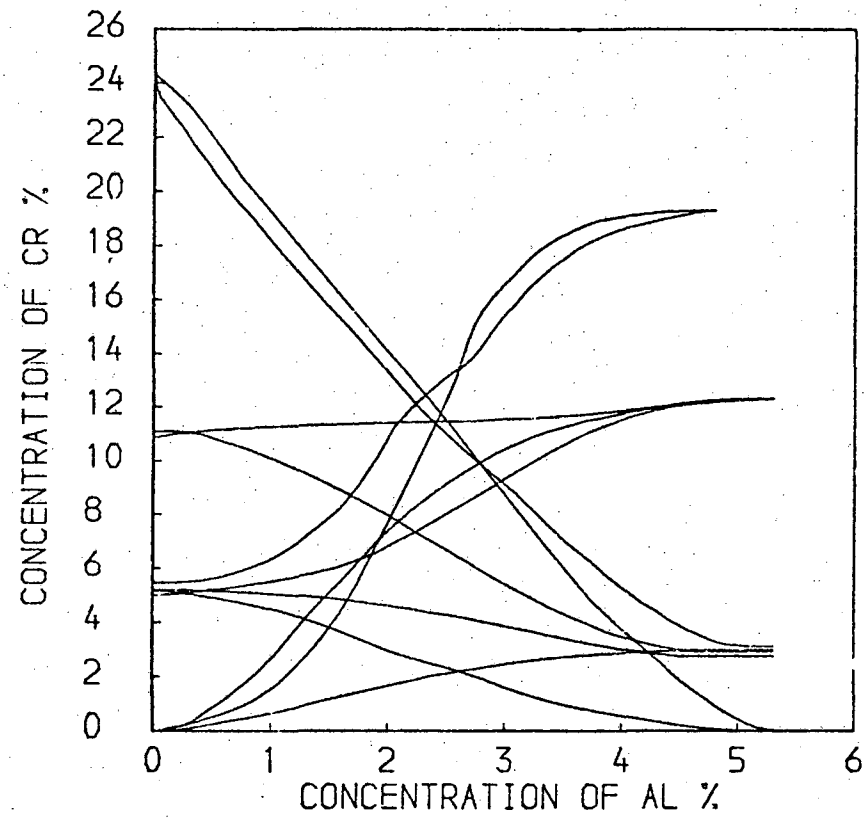

FIG. 4 Superposition of Diffusion Paths

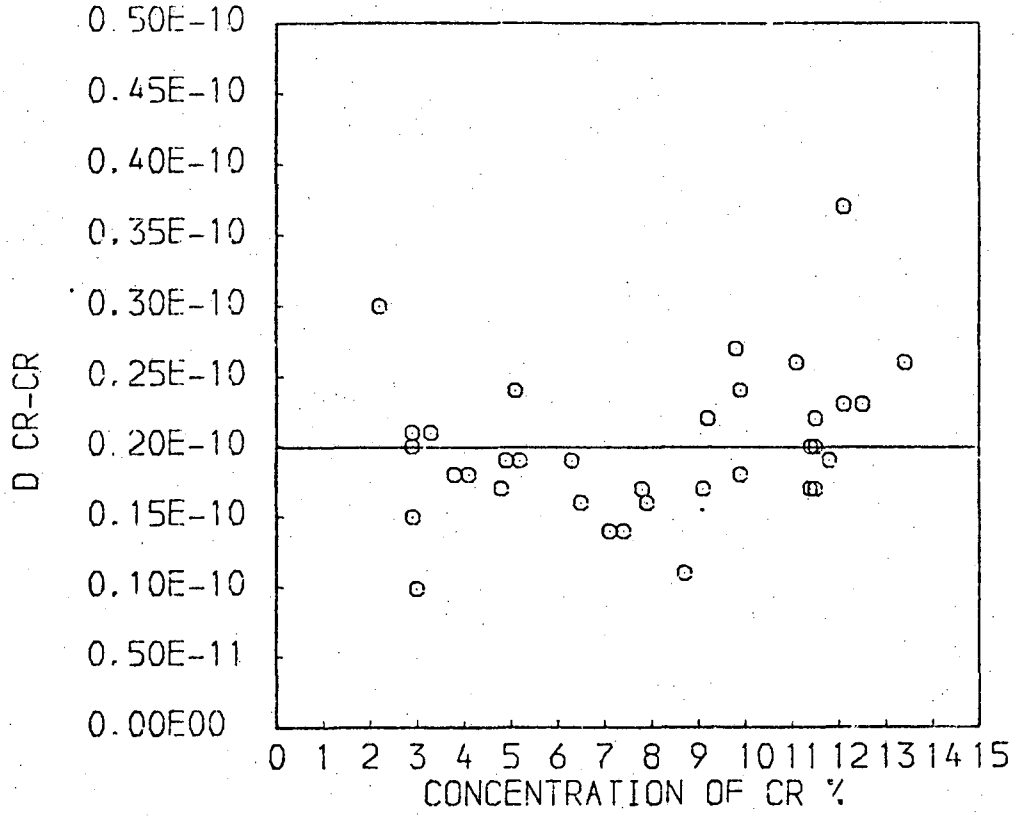

FIG. 5 : Variation of D_{CrCr} with Chromium Concentration

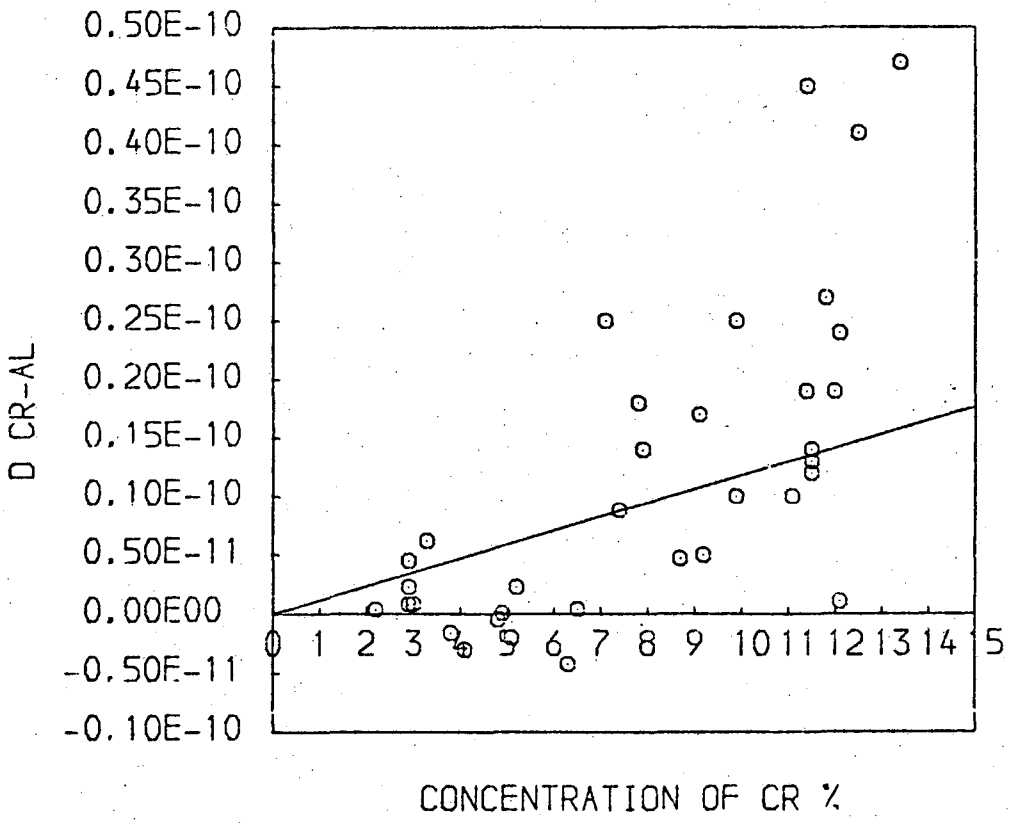

FIG. 6 : Variation of D_{CrAl} with Chromium Concentration

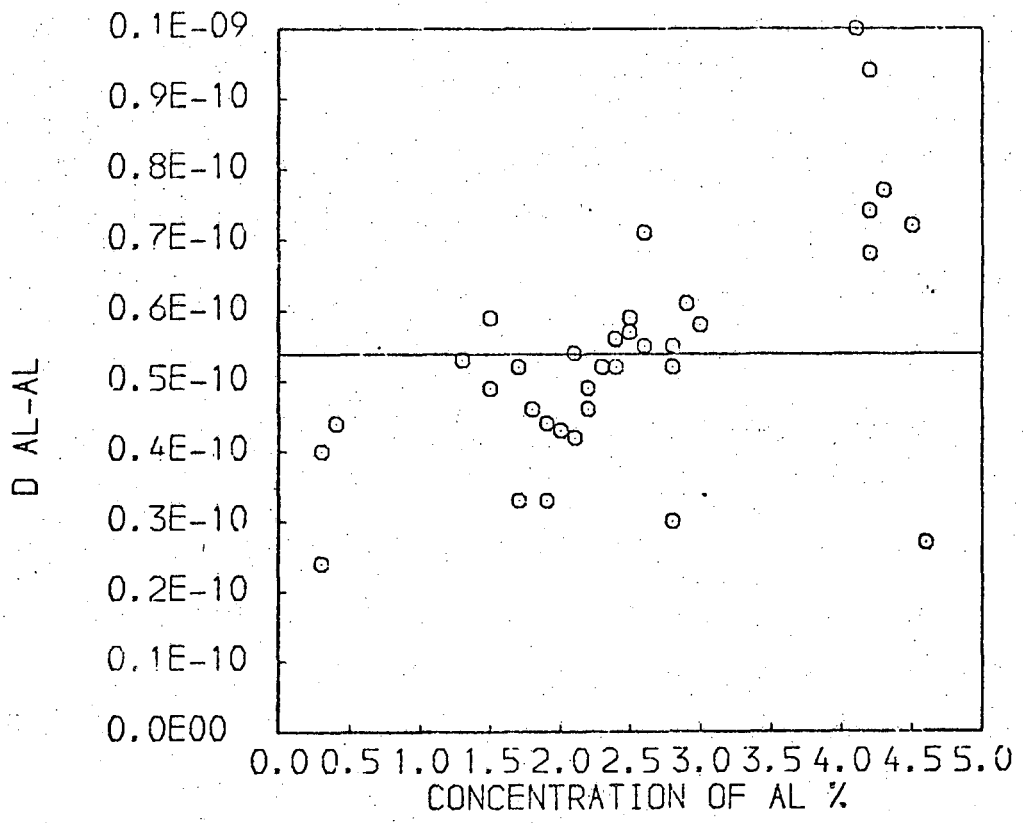

FIG. 7. Variation of D_{AlAl} with Aluminium Concentration

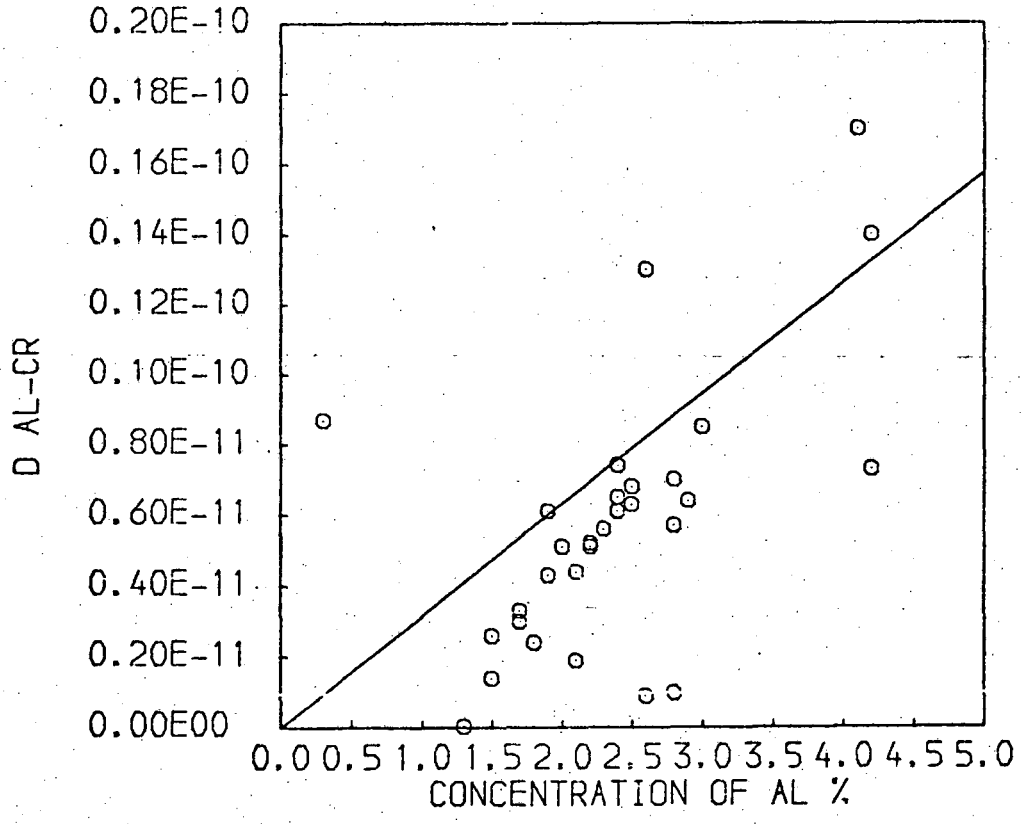

FIG. 8 Variation of D_{AlCr} with Aluminium Concentration

TECHNICAL INFORMATION DEPARTMENT
LAWRENCE BERKELEY LABORATORY
UNIVERSITY OF CALIFORNIA
BERKELEY, CALIFORNIA 94720